ACS APPLIED MATERIALS & INTERFACES

www.acsami.org

Research Article

Transfer-Free PZT Thin Films for Flexible Nanogenerators Derived from a Single-Step Modified Sol–Gel Process on 2D Mica

Shiyuan Liu, Deng Zou, Xinge Yu,* Zuankai Wang,* and Zhengbao Yang*

Cite This: *ACS Appl. Mater. Interfaces* 2020, 12, 54991–54999

Read Online

ACCESS | Metrics & More | Article Recommendations | Supporting Information

ABSTRACT: Piezoelectric materials enable emerging self-powered wearable and implantable devices. The sol–gel technology with the lowest cost for large-scale production has shown its potential for producing high-quality PZT thin films. However, fabricating PZT films with a sufficient thickness for different application scenarios requires a long and repeated coating and heat-treatment process. The traditional solution-based method usually requires at least 20 coating cycles to fabricate 2 μm-thick PZT thin films. To save cost and improve fabrication efficiency, we develop a simplified thin-film fabrication method assisted by PZT powder. The new method can fabricate 2 μm-thick PZT films in a single step, one spin coating and annealing. Experiments indicate that the powder-based PZT thin films have porous structures and outstanding piezoelectric performances. The measured d_{33} of the powder-based PZT thin film is 47 pm/V. Both solution-based and powder-based PZT thin films show high flexibility and good fatigue resistance. Furthermore, we explore 2D mica as the substrate and achieve the transfer-free fabrication of flexible PZT thin-film nanogenerators that effectively simplify the complicated physical or chemical thin-film lift-off processes. The nanogenerator prototypes demonstrate the capability of accurately monitoring dynamic responses of flexible and soft human tissues.

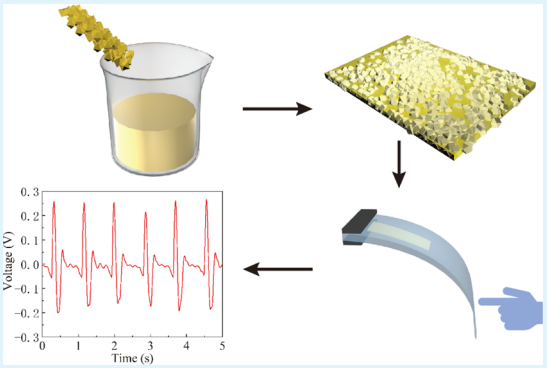

KEYWORDS: *single-step sol–gel preparation, PZT thin films, transfer-free, piezoelectric nanogenerators (PENGs), two-dimensional mica*

INTRODUCTION

Many electronic devices rely upon piezoelectric ceramic films, especially perovskite $Pb_1Zr_xTi_{1-x}O_3$ (PZT) that shows high piezoelectric effect,[1,2] excellent ferroelectric behavior,[3,4] and outstanding compatibility with semiconductors.[5] In the last decade, PZT films have been demonstrated as human-scale vibration energy harvesters,[6−8] piezoelectric nanogenerators (PENGs),[9−11] sensors,[12] and actuators.[13] PZT films have also been reported as essential components to serve as functional layers in microrobotics to monitor the robotic motion and sense the interface without external energy supply.[14] It has also been demonstrated in artificial skins with excellent mechanical stability to harvest the energy from human motion to provide plenty of power for other clinical diagnostics, physiological parameter monitoring, and human–machine interfaces.[15,16] These novel application potentials have opened the gate to apply piezoelectric films in advanced technological fields such as the internet of things[17] and artificial intelligence.[18]

To better integrate PZT films into flexible electronics, fabricating PZT films via micro-electromechanical systems has been widely studied. Technologies such as sol–gel processing,[9,10,19] rf-magnetron sputtering,[20,21] pulsed laser deposition,[22] and metal–organic chemical vapor deposition[23] have been successfully demonstrated to synthesize high-quality PZT films. Among all these techniques, the sol–gel method has received extensive attention because of its low cost and simple processing flow. A variety of hard substrates such as SiO_2/Si,[21] Al_2O_3,[9,24] and MgO[25] have been conducted to grow high-quality single-crystalline or polycrystalline and crack-free PZT films via the sol–gel method. For further flexible device fabrication, processes such as laser lift-off are required to transfer the thin film to target flexible substrates.[9,24,26] However, inevitable transfer processes and complicated coating and heating steps increase the difficulty of integrating PZT thin films into flexible electronics, specifically

- Most fabrications need special transfer processes, either etching[27] or laser lifting,[9,24,26] to obtain standalone PZT films. However, the high temperature of the laser and the separation of the interfaces between the thin film and the hard substrate have high possibility of damaging the thin film that affects the piezoelectric performance and dramatically increases the fabrication cost.

Received: September 21, 2020
Accepted: November 13, 2020
Published: November 25, 2020

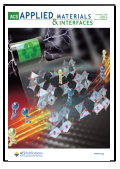

https://dx.doi.org/10.1021/acsami.0c16973
ACS Appl. Mater. Interfaces 2020, 12, 54991–54999

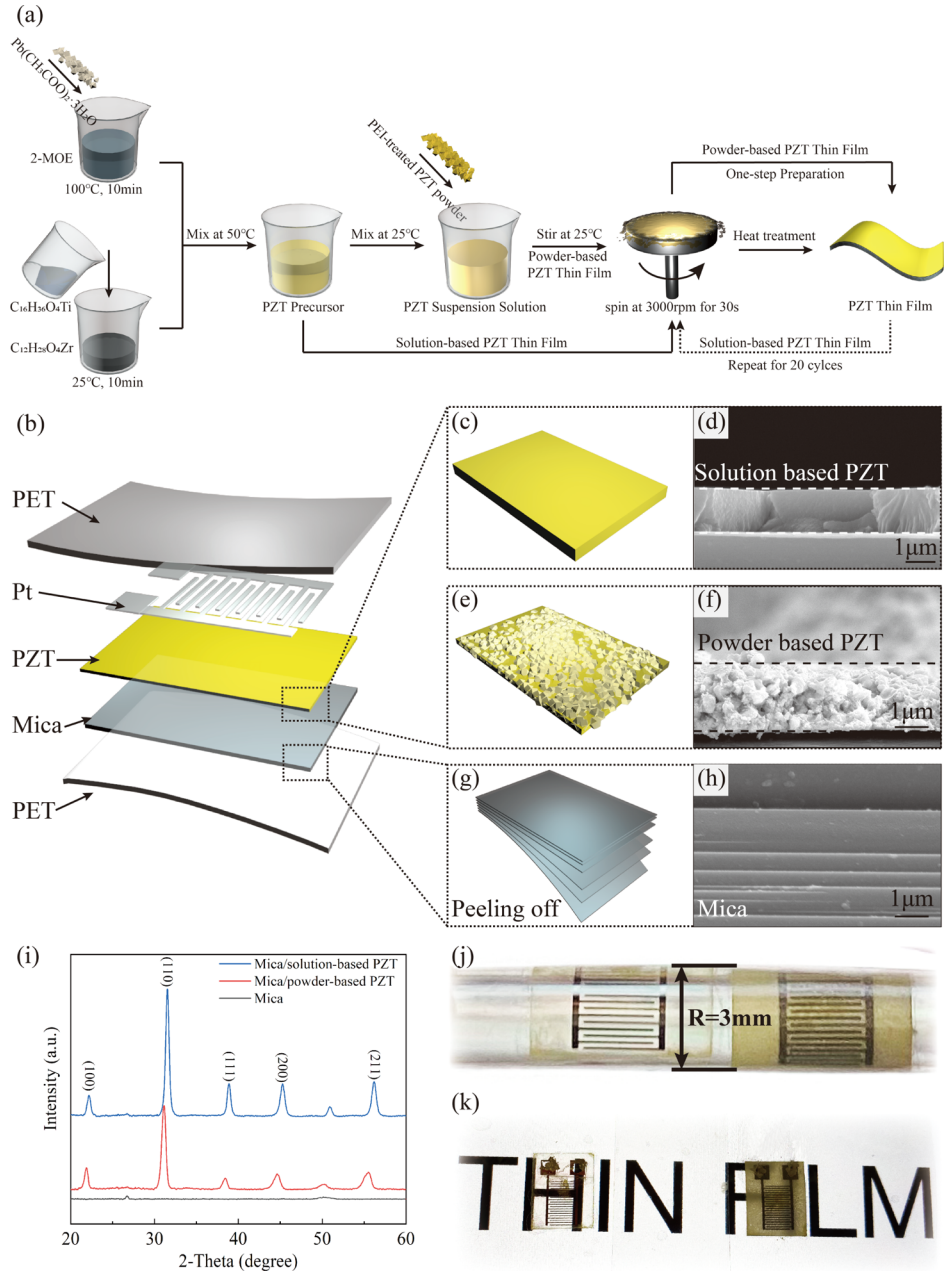

Figure 1. Preparation process of the PZT thin film-based PENG and the materials characterization of the PZT films. (a) Modified sol−gel preparation process of powder-based PZT thin films and solution-based PZT thin films. The powder-based PZT thin film only requires one coating and annealing process to achieve the desired thickness (2 μm), while traditional solution-based PZT thin films need at least 20 coating and heating cycles. (b) Structure of the PENG is PET/Pt/PZT/Mica/PET. (c,e,g) show the morphology of the solution-based PZT film, of the powder-based PZT film, and the peeling off of the mica substrate. (d,f,h) The cross-sectional SEM images of the solution-based PZT film, of the powder-based PZT film, and the peeling off of the mica substrate. (i) XRD patterns of the solution-based PZT, powder-based PZT, and the mica substrate. (j) shows the bending radius of the two PENGs and (k) transparency of the PENGs in optical images.

- The complicated coating and heating steps for 2 μm or thicker PZT films increase the possibility of cracks[28] and impede the mass production of PZT film-based devices.

To eliminate the barriers between PZT thin film mass production and applications in flexible electronics, we propose to use fluorophlogopite mica ($KMg_3(AlSi_3O_{10})F_2$), an artificial 2D layered structural silicate with superior chemical inertness, high thermal stability, and perfect mechanical strength, to grow PZT thin films for the fabrication of flexible PENGs. The specific properties of artificial mica are shown in Table S1 (Supporting Information). Because of the effect of the van der Waals force on the interlayer interaction, the bulk mica can be mechanically peeled off to a thickness less than 20 μm with adhesive tapes.[10] Compared with another opaque stainless steel, which is widely used as a substrate for flexible devices, the artificial mica has high light transmittance. These advantages allow thin films grown on mica to directly integrate into flexible optoelectronic devices.

To optimize the preparation process of PZT films and reduce the complexity caused by repeated coating, we added commercial PZT-5H powder into the PZT sol solution to increase the film thickness in a single coating process, which is

https://dx.doi.org/10.1021/acsami.0c16973
ACS Appl. Mater. Interfaces 2020, 12, 54991−54999

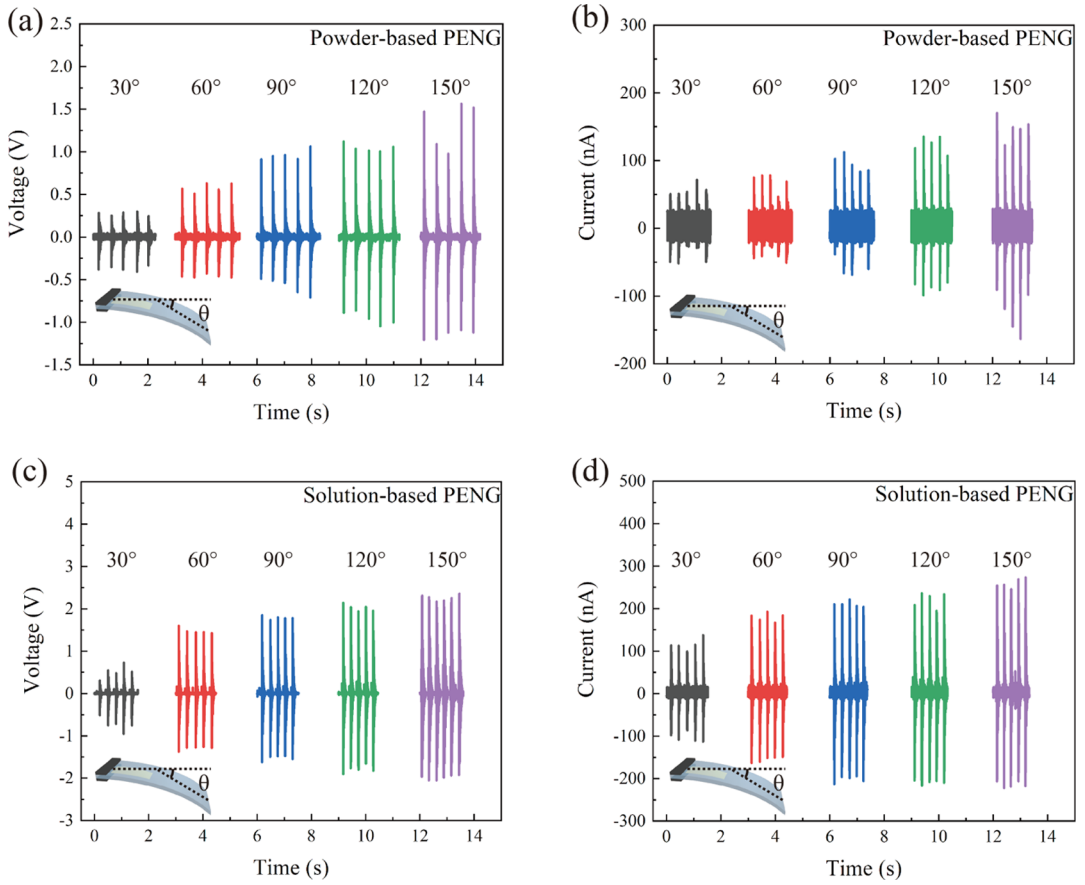

Figure 2. Piezoelectric performance of the PENGs in the bending−releasing mode. (a,b) show the open-circuit voltage and short-circuit current output of powder-based PENG releasing from different bending angles (30, 60, 90, 120, and 150°, respectively). (c,d) show the open-circuit voltage and short-circuit current output of solution-based PENG releasing from different bending angles.

developed from the traditional sol−slurry method.[29] The sol−slurry solution is commonly applied in spray coating and screen printing to fabricate thick films with a thickness larger than 10 μm. Polyethylenimine (PEI) as a surface-activated agent is added, allowing PZT powder to be better mixed with the PZT sol solution.[30] In the presence of the excessive amount of powder, only one cycle of film coating and heat treatment is needed to obtain a 2 μm-thick PZT film, while 20 procedures are required for pure sol solution-derived films in the traditional process. The sole sol solution-based PZT films and powder-based PZT films were directly fabricated as flexible PENGs without any transfer process to examine the piezoelectric performances. The mechanical stability of both PENGs allows them to endure 50,000 cycles under fatigue testing without compromising performances. The d_{33} of the powder-based PENG with 20 times simpler manufacturing process reaches 47 pm/V. The successful demonstration of human motion monitoring and energy harvesting illustrates the potential applications on flexible electronics.

RESULTS

PZT Thin Film Structures and Morphologies. The PZT thin film preparation process is illustrated in Figure 1a and the details have been shown in Methods. The structure of the fabricated PENGs is shown in Figure 1b. The Pt-based interdigital electrodes (IDEs) are used to harvest the electric potential from the PZT thin film, and the two layers of PET films serve as passivation and protection layers. To compare the performances of the PENG fabrication by different processes, two types of PZT films are presented. The PZT thin film prepared by the sole solution coating process has a uniform and smooth surface, as shown in Figure 1c,d. The thickness of the film is measured by scanning electron microscopy (SEM), and both types of PZT films reach 2 μm thickness. The concentration of the precursor solution used for preparing solution-based PZT films is 0.5 mol/L, and it requires at least 20 coating and baking cycles to increase the film thickness to 2 μm. Theoretically, a higher concentration will contribute to a larger thickness in one coating cycle; however, in this case, PZT films are prone to cracking during the heating treatment process because of the bubbles generated by solvent evaporation and the lattice mismatch between the film and the substrate.[31] To overcome this limitation, PZT powders with PEI activated are introduced into the precursor solution to form a uniform suspension, which is modified by the traditional fabrication process that combines PZT powders with solution to fabricate large-area films, has been used to obtain tens to hundreds of micrometers via spray and screen coating.[29] The PZT powder is excessively added with the weight ratio between powder and solution equating to 1:2, and in one coating round, the PZT film will reach around 2 μm, which is significantly efficient than sole solution-based film coating. The morphology of the powder-based PZT thin film is shown in Figure 1e,f. Compared to the solution-based PZT thin film, the powder-based film shows more porosity, and powders are distributed uniformly throughout the film. The

https://dx.doi.org/10.1021/acsami.0c16973
ACS Appl. Mater. Interfaces 2020, 12, 54991−54999

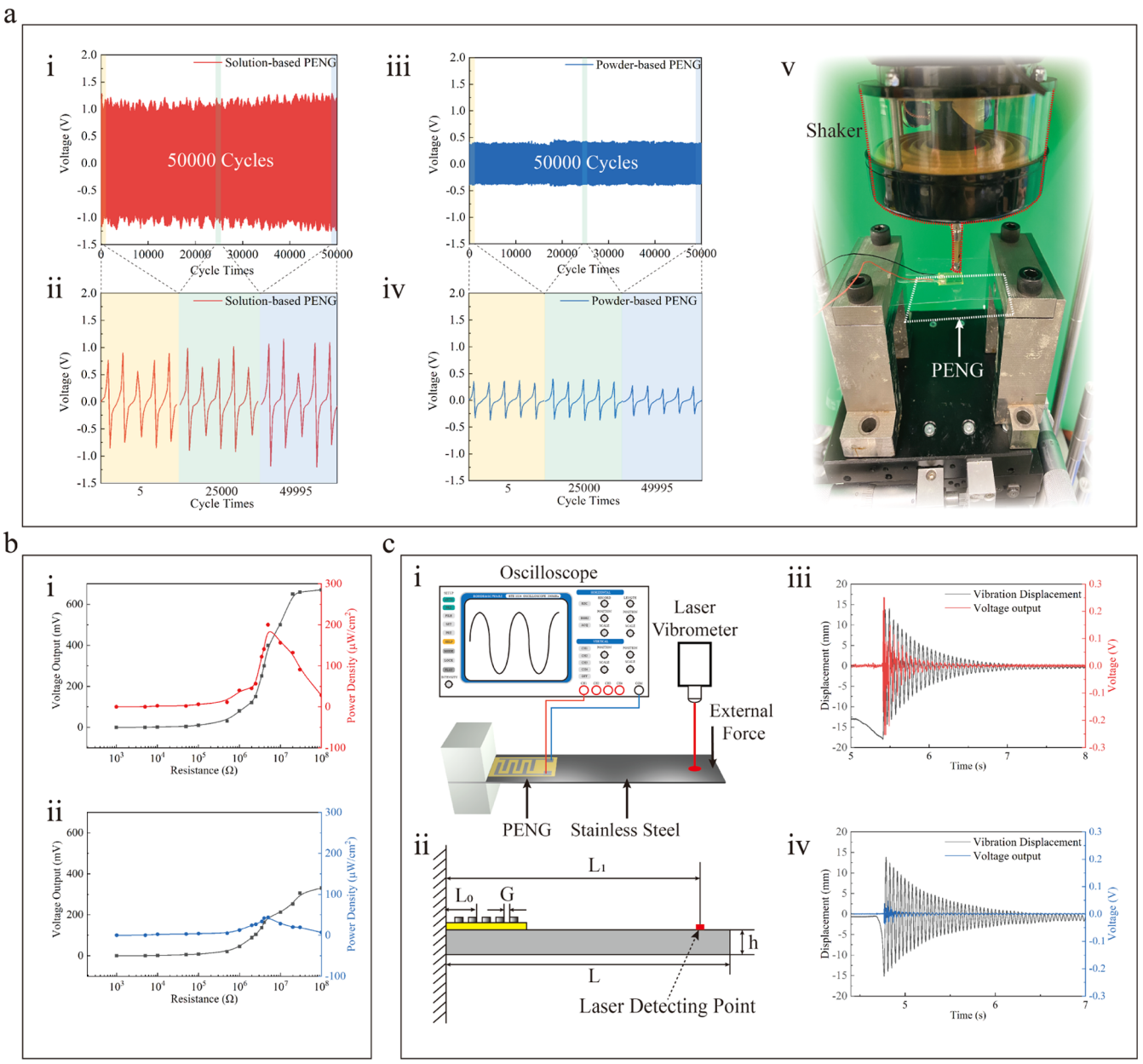

Figure 3. Piezoelectric performance characterizations of the solution-based and powder-based PENGs. (a) Voltage output from the fatigue test of (i,ii) solution-based PENG and (iii,iv) powder-based PENG. (b) shows the impedance matching results of the two types of PENGs. (c) (i,ii)d_{33} measurement system and (iii,iv) measuring signal samples of the two types of PENGs.

average size of the powder is 1.1 μm, and the particle size distribution of the PZT powder is derived by measuring the powders on the top surface of the powder-based film from the SEM image, as shown in Figure S1. To further compare the properties among different added amounts of PZT powder, the weight ratios of PZT powder/PZT solution with 1:1 and 1:10 are fabricated under the same condition and characterized individually, which are shown in Figure S2c,d. The cross-sectional SEM images show that the thickness of the three types of films are slightly different in one coating cycle, where the film with 1:1 weight ratio is 2.5 μm thick and that with 1:10 is 1.9 μm thick.

The two-dimensional mica is selected as the flexible and transparent substrate for PZT growth, as shown in Figure 1g,h. Because of the weak van der Waals interlayer interactions that can be easily peeled off between mica layers by mechanical exfoliation with tapes, the mica is peeled off to 20 μm by tapes to reach high flexibility. Therefore, PZT thin films grown on mica can be directly fabricated as flexible and transparent nanogenerators without extra laser lift-off or chemical etching processes that are ready to produce cracks on the films during the operation. To examine the crystal structure of the PZT films grown on mica substrates, grazing incidence X-ray diffraction (XRD) was implemented with the 2θ from 20 to 70°. Figure 1i illustrates XRD patterns of the mica substrate, mica/powder-based PZT, and mica/solution-based PZT. The (110) direction is the preferred crystal orientation for both types of PZT films, and the solution-based PZT film has higher peaks because of the existence of the porous structures in the powder-based PZT film. Compared to the solution-based PZT film, the characteristic peaks of the powder-based PZT film shift slightly to right, resulting from the bending of the flexible

https://dx.doi.org/10.1021/acsami.0c16973
ACS Appl. Mater. Interfaces 2020, 12, 54991−54999

film during the heat treatment process, which slightly affects the results of the XRD pattern. According to Figure S2a, the XRD patterns of the films with different amounts of powders are similar but different from that of the sole solution-based film, which indicates that the crystallinity of the film mainly depends on the added PZT powder. The optical image of the PENG prototypes in Figure 1j indicates that the fabricated PENGs are flexible that can be bent under the radius of curvature of 3 mm, and Figure 1k shows that the solution-based PZT film is transparent, while the powder-based one is semitransparent, and the background pattern "THIN FILM" can be viewed through the films.

Piezoelectric Performance Characterizations of PENGs. The 20 μm-thick mica substrate with high flexibility enables the direct application of PENGs based on PZT thin films. Figure 2 shows the electric output from the flexible PENG. The PENG is encapsulated by two layers of 100 μm-thick PET films to ensure the structural stability of PZT and the electrodes. To avoid the triboelectric effect when touching or tapping the surface of the PENG, the piezoelectric signal outputs from the powder-based PENG are examined by bending, as shown in Figure 2a,b. The PET is clamped by a customized fixture to form a cantilever beam structure with 20 mm width and 50 mm length. The 12 mm × 15 mm PZT film is placed at the fixed end of the cantilever. The oscilloscope records the PENG electric outputs including open-circuit voltage and short-circuit current generated by the spontaneous release from the different bending angles between the curvature of the fixed end and the free end. As the bending angles increase, the stress generated at the moment of release improved, which brings a higher strain rate and produces a higher piezoelectric output. According to the results, the amplitude voltages of the solution-based PENG are 0.3, 0.7, 1.0, 1.2, and 1.5 V under the releasing angle at 30, 60, 90, 120, and 150°, respectively, and the currents are 60, 80, 110, 130, and 160 nA, respectively. The electric outputs from solution-based PENG by the same excitation method are shown in Figure 2c,d. The solution-based PENG has a higher electric output. At 15°, the amplitude voltage is 2.5 V and the amplitude current is 280 nA. The reason for the lower electric output of powder-based PENG is that the existence of a large number of holes introduced by the PZT powders reduces the uniformity and influences the piezoelectric performance of the film. Besides, the magnetron sputtering-deposited Pt-based IDEs cannot grow on the film surface uniformly, which increases the internal impedance and affects the output electric potential. Therefore, the powder-based PENGs are much easier to be fabricated, while the piezoelectric performances of the solution-based PENGs are better. The performances among different amounts of added PZT powder are shown in Figure S3. They all exhibit around 0.5 V output while bending at 60°, which indicates that the different amount of excessive PZT powder will not significantly affect the piezoelectric performances.

To examine the life cycles of the two types of PENG, a fatigue testing experiment has been conducted, as shown in Figure 3a. In this experiment, the PENGs are cut into 20 mm width and 50 mm length, and the PZT films are placed at the center of the PET film. The two short sides are clamped by two parallel customized fixtures, and the PZT film is tapped by a shaker with 30 Hz. The detailed experiment setups are shown in Figure 3aiii. After 50,000 cycles, the voltage outputs of the two types of PENGs are generally stable, where the solution-based PENG is around 1 V in Figure 3ai and the powder-based PENG is around 0.4 V in Figure 3aii. The interfaces of the tapping area of the powder-based PENG before and after the fatigue test are shown in Figure S4. Fractures and impressions are barely seen on the surface. The good stability relies on the protection from the PET passivation film.

To further evaluate the output power of the PENG, the external load resistances ranging from 1 kΩ to 100 MΩ are applied and the oscilloscope is used to record the electric potential difference on the external load (see as Figure 3b). The output power is calculated by

$$P_i = {V_{out}}^2/R_i \tag{1}$$

As a result, the two types of PENGs have a similar tendency for the instantaneous output voltage and power, and they reach the highest power density at 7 MΩ with 12.5 and 3.2 μW/cm^2, respectively. It is worth noting that in the impedance matching experiment, the piezoelectric outputs are generated by finger-tapping on the free end of the cantilever PENG, as shown in Figure 2. Thus, in this case, the results can only qualitatively characterize the power of PENG, while the exact value requires more complicated dynamics experiments and calculations.

To better characterize the piezoelectric performances of the PENGs, d_{33} was calculated, as shown in Figure 3c. Because of the difficulty in obtaining the precise value of d_{33} of PZT thin films with IDEs from the conventional d_{33} meter, we established a cantilever system to evaluate the d_{33} value by a simplified system. First, the IDEs are regarded as parallel electrodes that are inserted into the PZT film, so we have

$$C = \varepsilon\frac{A}{G} = \varepsilon\frac{tl}{G} \tag{2}$$

where C is the capacitance of the PZT film. ε is the permittivity of the PZT film at a low frequency (i.e., 1000 Hz), which can be measured via a ferroelectric analyzer. l is the length of each electrode finger, t is the thickness of the PZT film, and G is the gap between two electrodes. Q is the charge generated from two electrodes and can be calculated by the multiplication of electrical displacement D_3 and effective electrode area A

$$Q = D_3A = d_{33}T_3lt \tag{3}$$

The measured output voltage V can be calculated by

$$V = \frac{Q}{C} = \frac{D_3}{\varepsilon}G \tag{4}$$

Therefore, d_{33} can be expressed as

$$d_{33} = \frac{\varepsilon V}{GT_3} \tag{5}$$

The average stress between two electrodes, T_3, can be derived from a cantilever model, which has been shown in Figure 3cii. L, b, and h represent the length, width, and thickness of the cantilever, respectively. The laser vibrometer is used to record the real-time displacement of the free-end vibration driven by a spontaneous force F. Here, we assume that the effective length of the PENG is L_0, and the distance between the electrodes and the fixed end is x. The moment on the cantilever can be calculated by

$$M_x = F(L - x) \tag{6}$$

Thus, the average stress T_3between two electrode fingers can be derived by

https://dx.doi.org/10.1021/acsami.0c16973
ACS Appl. Mater. Interfaces 2020, 12, 54991−54999

Table 1. Comparison of PZT-Based Piezoelectric nanogenerators[a]

materials	voltage (V)	current (nA)	current density (μ A/cm^2)	power (nW)	power density (μ W/cm^2)	transparency	transfer process	thickness (μm)	fabrication process
thin film[12]	0.3	10[b]	0.32			opaque	free	2	>10 steps
thin film[33]	0.12	2290	1.145[b]	143	0.072	opaque	free	3	10 steps
thin film[6]	0.69			5600		opaque	free	1	10 steps
thin film[34]	2	300[b]	2.2	359[b]	2.64[b]	semitransparent	etching	0.3	6 steps
thin film[24]	0.28	30	0.03	8.4[b]	0.0084	transparent	laser lift-off	1	RF-sputter
thin film[35]	3.8	140			1.2	semitransparent	etching	0.5	electron beam
nanofiber[11]	1.63			30		opaque	etching		electron spin
nanowires[36]	0.6	3.95	3.29[b]			transparent	free	150	electron spin
composite[16]	1.2	2600	0.52[b]	720[b]	0.14[b]	opaque	free	1200	dispersion
solution-based thin film[c]	2.5	280	10.9	320	12.5	transparent	free	2	20 steps
powder-based thin film[c]	1.5	150	5.9	80	3.2	semitransparent	free	2	single step

[a]Superiorities of the PZT-Based nanogenerators from our method are shown in the table, specifically: (1) relatively high current density and power density; (2) only one step is needed to deposit 2 μm-thickness PZT thin film; (3) no transfer process is required to fabricate transparent and flexible devices. [b]Value is calculated from the data in the literature. [c]Data in this work.

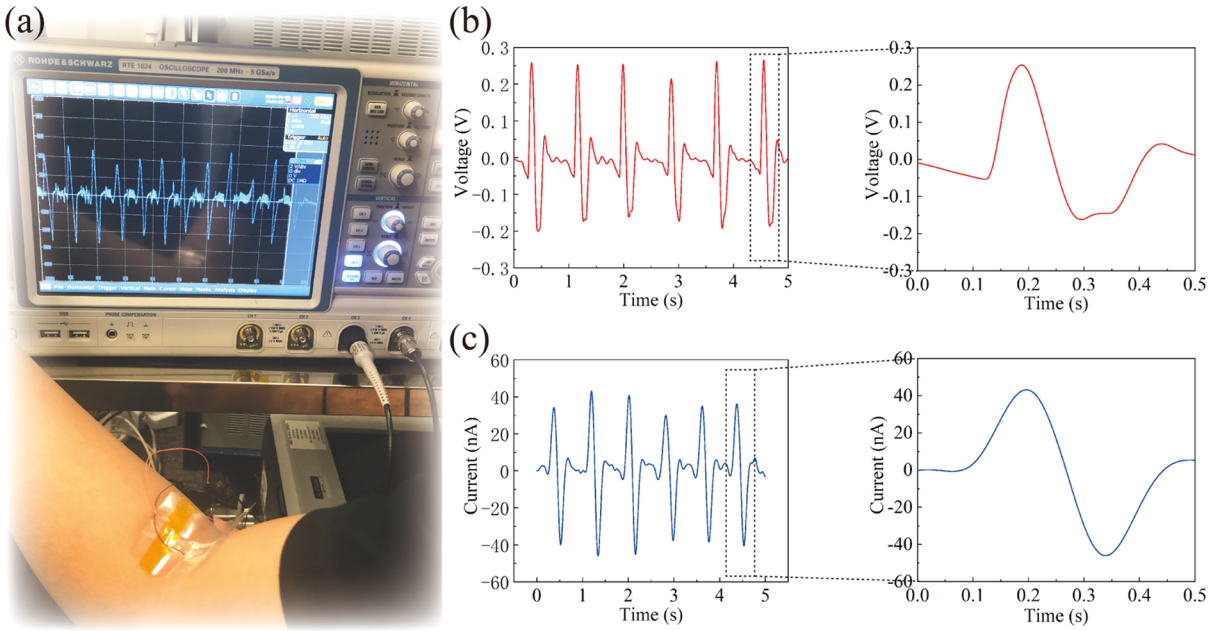

Figure 4. Developed PENG used as a biosensor for monitoring human arm motion. (a) Optical image of the testing system. (b) Voltage and (c) current output signal generated from the bending and releasing motions.

$$T_3 = \frac{\overline{M_x}}{I_z} = \frac{\int_0^{L_0} \frac{M_x}{L_0} dx}{I_z} = \frac{3F(2L - L_0)}{bh^2} \quad (7)$$

The spontaneous force F can be calculated from the measured displacement ν

$$F = \frac{6EI\nu}{(3L - L_1){L_1}^2} \quad (8)$$

where L_1 is the distance between the measured point and the fixed end. E and I are Young's modulus and moment of inertia of the cantilever, respectively.

Finally, we derive the value of d_{33} by applying eqs 5, 7, and 8. The average d_{33} of the solution-based PENG is 130 pm/V and that of the powder-based PENG is 47 pm/V. The recorded signals of the displacement and the output voltage for each type of sample have been shown in Figure 3ciii,iv. Both the voltage output signals and the displacement signals damp with time.

The solution-based PZT thin film with better quality can be obtained by 20 step-film coating processes, while the powder-based PZT will only need one step to achieve the same thickness and flexibility. Both processing techniques do not require an additional "transfer" process for further fabrication as sensors or energy harvesters. Both types of PZT films exhibit high power density and power output. Although the power density of the powder-based PZT thin film is not higher than that of solution-based PZT, it still shows competitive output compared with those of previous PZT-related works, as listed in Table 1.

To demonstrate its potential use as a sensor or PENG on the human body, we attached the powder-based PENG on the human elbow joint, as shown in Figure 4. Driven by the elbow joint, the PENG will bend and relax with the upper and lower

https://dx.doi.org/10.1021/acsami.0c16973
ACS Appl. Mater. Interfaces 2020, 12, 54991−54999

arms. The bending arms induce a positive electric signal and the release induces a negative electric signal from the PENG. The root-means-square output voltage V_{RMS} is 85 mV, and the root-means-square current I_{RMS} is 29 nA. The recorded PENG response to the arm motion has been attached as Supporting Information Video S1.

CONCLUSIONS

We successfully fabricated two types of PENGs via a pure solution route and powder assistant method by sol−gel techniques. The process of fabricating powder-based PZT film can reduce the preparation time by least 20 times compared to traditional solution-based PZT. Furthermore, the complicated and expensive transfer process is replaced by the simple mechanical exfoliation of mica substrate by tapes for the fabrication of devices such as PENGs and sensors. The piezoelectric performance of the solution-based PZT film is better than that of the powder-based PZT film, which can be explained by the material characterization results that the density and crystallinity of the solution-based PZT film are better than those of the powder-based one. In bending−releasing mode at 150°, open-circuit voltage outputs are 2.5 and 1.5 V, the short-circuit current densities are 10.9 and 5.9 $\mu A/cm^2$, and the power densities reach 12.5 and 3.2 $\mu W/cm^2$, respectively. Both types of PENGs remain mechanically and electrically stable after 50,000 testing cycles. Flexible and transparent PENGs can be widely used in artificial skins, energy harvesters, and force sensors.

METHODS

Fabrication of PZT Solution and Powder-Based Films. In this study, we adopt the sol−gel technique to obtain the $Pb_{1.1}Zr_{0.52}Ti_{0.48}O_3$ thin film with 10% excess Pb to compensate for the volatilization of PbO at high temperature during the annealing process.[32] The overall PZT thin-film preparation processes have been schematically concluded, as shown in Figure 1a. A total of 5 g of lead(II) acetate trihydrate $(Pb(CH_3COOH)_2)\cdot 3H_2O$ (TCI) is first dissolved in 2-methoxyethanol (Alfa Aesar, 99%) at 130 °C for 12 h and mixed by magnetic stirring. When it is completely dissolved, the solution is cooled down to room temperature. A total of 3.848 g of zirconium(IV) *n*-propoxide ($C_{12}H_{28}O_4Zr$, TCI, 70 wt % in 1-propanol) is mixed with 2.432 g of titanium(IV) butoxide ($C_{16}H_{36}O_4Ti$, TCI, 99%) in another container. Then, zirconium(IV) *n*-propoxide and titanium(IV) butoxide are added to lead(II) acetate trihydrate solution, heated up to 90 °C, and diluted by 2-methoxyethanol to 0.5 M with stirring for 6 h in the atmosphere. The as-prepared solution was stored in the atmosphere at least 3 days for aging. Finally, a transparent and pale-yellow PZT sol with a certain viscosity is obtained.

For powder-based films, PZT-5H powder (Xi'an Yisheng Electronic Ltd.) is first mixed with 10 mL of polyethylenimine (PEI, Aldrich) water solution with a mass ratio 1:5 completely and stirred at room temperature for 30 min, followed by centrifugation at 3000 rpm for 10 min to separate the powder and PEI solution. The treated PZT powder is ready to form a uniform suspension solution when mixing with the as-prepared PZT sol with mass ratios 1:1, 1:2, and 1:10, which could be maintained stable for several hours. It is worth noting that the suspension solution should be stirred well before the thin-film coating. For a sole solution-based PZT film, the coating process has to be repeated at least 20 times to reach the same thickness as the powder-based film.

The thin-film grown substrate artificial mica (Taiyuan Fluorophlogopite Mica Company Ltd.) is ultrasonically cleaned by ethanol for 10 min. PZT films are derived by spin-coating at 3000 rpm for 30 s on artificial mica substrates, which is first mechanically exfoliated by a tape to 20 μm to enhance the flexibility. After coating, the sample is directly heated on a hot plate at 400 °C for at least 10 min for drying and volatilizing organic matter. This procedure is repeated 20 times to obtain the desired thickness for the sole solution-based PZT thin film. Only one coating step that drops the aforementioned suspension solution and spin-coating with 3000 rpm for 30 s is enough. Thereafter, the sample is placed in a muffle furnace, heated to 700 °C with 1 h, annealed for 30 min, and cooled down in the furnace.

Fabrication of Piezoelectric Nanogenerators. The Pt-based IDEs with 150 μm finger width, 300 μm finger spacing, 8 mm finger length, and 100 nm thickness are deposited via magnetron sputtering (Q150TS) onto the surface of PZT thin film. To protect the films and electrode structure, two 100 μm-thick layers of ethylene vinyl acetate/polyethylene terephthalate (EVA/PET, Lei Sheng Ltd.) are stamped at 100 °C onto both sides of PZT/mica films. The two wires are connected to IDE through the conductive silver paste. Thereafter, PZT films are polarized at 140 °C under 100 kV/cm for 30 min.

Materials Characterization of PZT Films. The cross-sectional morphologies of two types of PZT films and mica substrates are examined by SEM (FEI Quanta 450). The crystal structures of the materials are characterized by X-ray diffraction (XRD, Rigaku SmartLab) via grazing-incident small-angle scattering mode.

Piezoelectric Performance Characterization. To identify the piezoelectric performance, the open-circuit output voltages were measured by an oscilloscope (Rohde & Schwarz RTE1024), and the short-circuit current was measured by the current amplifier (Stanford Research SR570). In the d_{33} measurement experiment, the laser vibrometer (Polytec NLV-2500) is used to record the vibration displacement in real time.

Data Availability. All data needed to evaluate the conclusions in this paper are present in the paper and/or Supporting Information Additional data and raw data are available upon request from the authors.

ASSOCIATED CONTENT

Supporting Information

The Supporting Information is available free of charge at https://pubs.acs.org/doi/10.1021/acsami.0c16973.

Characteristic of the powder-based PZT thin film, properties of PZT films with three different weight percentage of powder, comparison of the piezoelectric outputs from bending−releasing mode of three different powder weight percentages of PZT films, optical microscopy images of the surface of the powder-based PENG, and basic properties of fluorophlogopite mica (PDF)

Real-time human motion detection (MP4)

AUTHOR INFORMATION

Corresponding Authors

Xinge Yu − *Department of Biomedical Enginee Ring, City University of Hong Kong, Hong Kong 999077, China;* orcid.org/0000-0003-0522-1171; Email: xingeyu@cityu.edu.hk

Zuankai Wang − *Department of Mechanical Engineering, City University of Hong Kong, Hong Kong 999077, China;* orcid.org/0000-0002-3510-1122; Email: zuanwang@cityu.edu.hk

Zhengbao Yang − *Department of Mechanical Engineering, City University of Hong Kong, Hong Kong 999077, China; Shenzhen Research Institute of City University of Hong Kong, Shenzhen 518057, China;* orcid.org/0000-0001-5075-0457; Email: zb.yang@cityu.edu.hk

https://dx.doi.org/10.1021/acsami.0c16973
ACS Appl. Mater. Interfaces 2020, 12, 54991−54999

Authors

Shiyuan Liu − *Department of Mechanical Engineering, City University of Hong Kong, Hong Kong 999077, China;* orcid.org/0000-0003-0966-5589

Deng Zou − *Department of Mechanical Engineering, City University of Hong Kong, Hong Kong 999077, China*

Complete contact information is available at: https://pubs.acs.org/10.1021/acsami.0c16973

Funding

We acknowledge the financial support from the Early Career Scheme from the Research Grants Council of Hong Kong (project no. 21210619), National Natural Science Foundation of China (no. 11902282), and the City University of Hong Kong (no. 9610390).

Notes

The authors declare no competing financial interest.

REFERENCES

(1) Yang, Z.; Zhou, S.; Zu, J.; Inman, D. High-Performance Piezoelectric Energy Harvesters and Their Applications. *Joule* **2018**, *2*, 642−697.

(2) Liu, Y.; Wang, L.; Zhao, L.; Yu, X.; Zi, Y. Recent Progress on Flexible Nanogenerators toward Self-powered Systems. *InfoMat* **2020**, *2*, 318−340.

(3) Muralt, P. Ferroelectric Thin Films for Micro-Sensors and Actuators: A Review. *J. Micromech. Microeng.* **2000**, *10*, 136.

(4) Jiang, J.; Bitla, Y.; Huang, C.; Do, T. H.; Liu, H.; Hsieh, Y.; Ma, C.; Jang, C.; Lai, Y.; Chiu, P.; Wu, W.; Chen, Y. Flexible Ferroelectric Element Based on van Der Waals Heteroepitaxy. *Sci. Adv.* **2017**, *1*, No. e1700121.

(5) Trolier-McKinstry, S.; Muralt, P. Thin Film Piezoelectrics for MEMS. *J. Electroceram.* **2004**, *12*, 7−17.

(6) Won, S. S.; Seo, H.; Kawahara, M.; Glinsek, S.; Lee, J.; Kim, Y.; Jeong, C. K.; Kingon, A. I.; Kim, S.-H. Flexible Vibrational Energy Harvesting Devices Using Strain-Engineered Perovskite Piezoelectric Thin Films. *Nano Energy* **2019**, *55*, 182−192.

(7) Wang, B.; Luo, X.; Liu, Y.; Yang, Z. Thickness-Variable Composite Beams for Vibration Energy Harvesting. *Compos. Struct.* **2020**, *244*, 112232.

(8) Gong, Y.; Shan, X.; Luo, X.; Pan, J.; Xie, T.; Yang, Z. Direction-Adaptive Energy Harvesting with a Guide Wing under Flow-Induced Oscillations. *Energy* **2019**, *187*, 115983.

(9) Park, K.-I.; Son, J. H.; Hwang, G.-T.; Jeong, C. K.; Ryu, J.; Koo, M.; Choi, I.; Lee, S. H.; Byun, M.; Wang, Z. L.; Lee, K. J. Highly-Efficient, Flexible Piezoelectric PZT Thin Film Nanogenerator on Plastic Substrates. *Adv. Mater.* **2014**, *26*, 2514−2520.

(10) Wang, D.; Yuan, G.; Hao, G.; Wang, Y. All-Inorganic Flexible Piezoelectric Energy Harvester Enabled by Two-Dimensional Mica. *Nano Energy* **2018**, *43*, 351−358.

(11) Chen, X.; Xu, S.; Yao, N.; Shi, Y. 1.6 V Nanogenerator for Mechanical Energy Harvesting Using PZT Nanofibers. *Nano Lett.* **2010**, *10*, 2133−2137.

(12) Ko, Y. J.; Kim, D. Y.; Won, S. S.; Ahn, C. W.; Kim, I. W.; Kingon, A. I.; Kim, S.-H.; Ko, J.-H.; Jung, J. H. Flexible Pb (Zr0. 52Ti0. 48) O3 Films for a Hybrid Piezoelectric-Pyroelectric Nanogenerator under Harsh Environments. *ACS Appl. Mater. Interfaces* **2016**, *8*, 6504−6511.

(13) Niu, X.; Jia, W.; Qian, S.; Zhu, J.; Zhang, J.; Hou, X.; Mu, J.; Geng, W.; Cho, J.; He, J.; Chou, X. High-Performance PZT-Based Stretchable Piezoelectric Nanogenerator. *ACS Sustain. Chem. Eng.* **2018**, *7*, 979−985.

(14) Lu, H.; Hong, Y.; Yang, Y.; Yang, Z.; Shen, Y. Battery-Less Soft Millirobot That Can Move, Sense, and Communicate Remotely by Coupling the Magnetic and Piezoelectric Effects. *Adv. Sci.* **2020**, *7*, 2000069.

(15) Liu, Y.; Wang, L.; Zhao, L.; Yao, K.; Xie, Z.; Zi, Y.; Yu, X. Thin, Skin-Integrated, Stretchable Triboelectric Nanogenerators for Tactile Sensing. *Adv. Electron. Mater.* **2019**, *6*, 1901174.

(16) Liu, Y.; Zhao, L.; Wang, L.; Zheng, H.; Li, D.; Avila, R.; Lai, K. W. C.; Wang, Z.; Xie, Z.; Zi, Y.; Yu, X. Skin-Integrated Graphene-Embedded Lead Zirconate Titanate Rubber for Energy Harvesting and Mechanical Sensing. *Adv. Mater. Technol.* **2019**, *4*, 1900744.

(17) Wang, Y.; Yang, Z.; Li, P.; Cao, D.; Huang, W.; Inman, D. J. Energy Harvesting for Jet Engine Monitoring. *Nano Energy* **2020**, *75*, 1 04853.

(18) Jung, Y. H.; Hong, S. K.; Wang, H. S.; Han, J. H.; Pham, T. X.; Park, H.; Kim, J.; Kang, S.; Yoo, C. D.; Lee, K. J. Flexible Piezoelectric Acoustic Sensors and Machine Learning for Speech Processing. *Adv. Mater.* **2019**, *32*, 1904020.

(19) Yang, Y.; Gao, W.; Xie, Z.; Wang, Y.; Yuan, G.; Liu, J. M. An All-Inorganic, Transparent, Flexible, and Nonvolatile Resistive Memory. *Adv. Electron. Mater.* **2018**, *4*, 1800412.

(20) Yeo, H. G.; Xue, T.; Roundy, S.; Ma, X.; Rahn, C.; Trolier-McKinstry, S. Strongly (001) Oriented Bimorph PZT Film on Metal Foils Grown by Rf-Sputtering for Wrist-Worn Piezoelectric Energy Harvesters. *Adv. Funct. Mater.* **2018**, *28*, 1801327.

(21) Ledermann, N.; Muralt, P.; Baborowski, J.; Gentil, S.; Mukati, K.; Cantoni, M.; Seifert, A.; Setter, N. {1 0 0}-Textured, Piezoelectric Pb(ZrxTi1-x)O3 Thin Films for MEMS: Integration, Deposition and Properties. *Sens. Actuators, A* **2003**, *105*, 162−170.

(22) Qi, H.; Xia, X.; Zhou, C.; Xiao, P.; Wang, Y.; Deng, Y. Ferroelectric Properties of the Flexible Pb(Zr0.52Ti0.48)O3 Thin Film on Mica. *J. Mater. Sci.: Mater. Electron.* **2020**, *31*, 3042−3047.

(23) Izyumskaya, N.; Alivov, Y.-I.; Cho, S.-J.; Morkoç, H.; Lee, H.; Kang, Y.-S. Processing, Structure, Properties, and Applications of PZT Thin Films. *Crit. Rev. Solid State Mater. Sci.* **2007**, *32*, 111−202.

(24) Do, Y. H.; Jung, W. S.; Kang, M. G.; Kang, C. Y.; Yoon, S. J. Preparation on Transparent Flexible Piezoelectric Energy Harvester Based on PZT Films by Laser Lift-off Process. *Sens. Actuators, A* **2013**, *200*, 51−55.

(25) Chidambaram, N.; Balma, D.; Nigon, R.; Mazzalai, A.; Matloub, R.; Sandu, C. S.; Muralt, P. Converse Mode Piezoelectric Coefficient for Lead Zirconate Titanate Thin Film with Interdigitated Electrode. *J. Micromech. Microeng.* **2015**, *25*, 045016.

(26) Park, D. Y.; Joe, D. J.; Kim, D. H.; Park, H.; Han, J. H.; Jeong, C. K.; Park, H.; Park, J. G.; Joung, B.; Lee, K. J. Self-Powered Real-Time Arterial Pulse Monitoring Using Ultrathin Epidermal Piezoelectric Sensors. *Adv. Mater.* **2017**, *29*, 1702308.

(27) Dufay, T.; Guiffard, B.; Seveno, R.; Ginestar, S.; Thomas, J.-C. Flexible PZT Thin Film Transferred on Polymer Substrate. *Surf. Coat. Technol.* **2018**, *343*, 148−152.

(28) Zhu, W.; Wang, Z.; Zhao, C.; Tan, O. K.; Hng, H. H. Low Temperature Processing of Nanocrystalline Lead Zirconate Titanate (PZT) Thick Films and Ceramics by a Modified Sol-Gel Route. *Jpn. J. Appl. Phys.* **2002**, *41*, 6969.

(29) Barrow, D. A.; Petroff, T. E.; Tandon, R. P.; Sayer, M. Characterization of Thick Lead Zirconate Titanate Films Fabricated Using a New Sol Gel Based Process. *J. Appl. Phys.* **1997**, *81*, 876−881.

(30) Lee, E. J.; Kim, T. Y.; Kim, S.-W.; Jeong, S.; Choi, Y.; Lee, S. Y. High-Performance Piezoelectric Nanogenerators Based on Chemically-Reinforced Composites. *Energy Environ. Sci.* **2018**, *11*, 1425−1430.

(31) Muralt, P.; Maeder, T.; Sagalowicz, L.; Hiboux, S.; Scalese, S.; Naumovic, D.; Agostino, R. G.; Xanthopoulos, N.; Mathieu, H. J.; Patthey, L.; Bullock, E. L. Texture Control of $PbTiO_3$ and Pb (Zr, Ti)O_3 Thin Films with TiO 2 Seeding. *J. Appl. Phys.* **1998**, *83*, 3835−3841.

(32) Chen, Z.; Zeng, Y.; Yang, C.; Yang, B. PbO Volatilization and Annealing Conditions Investigation of Pb (Zr0. 52Ti0. 48) O3 Thin Films Fabricated by Sol−Gel Method. *Mater. Sci. Eng. B* **2005**, *123*, 143−148.

(33) Seveno, R.; Carbajo, J.; Dufay, T.; Guiffard, B.; Thomas, J. C. Flexible PET/Al/PZT/Al/PET Multi-Layered Composite for Low Frequency Energy Harvesting. *J. Phys. D Appl. Phys.* **2017**, *50*, 165502.

(34) Kwon, J.; Seung, W.; Sharma, B. K.; Kim, S.-W.; Ahn, J.-H. A High Performance PZT Ribbon-Based Nanogenerator Using Graphene Transparent Electrodes. *Energy Environ. Sci.* **2012**, *5*, 8970−8975.
(35) Dagdeviren, C.; Yang, B. D.; Su, Y.; Tran, P. L.; Joe, P.; Anderson, E.; Xia, J.; Doraiswamy, V.; Dehdashti, B.; Feng, X.; Lu, B.; Poston, R.; Khalpey, Z.; Ghaffari, R.; Huang, Y.; Slepian, M. J.; Rogers, J. A. Conformal Piezoelectric Energy Harvesting and Storage from Motions of the Heart, Lung, and Diaphragm. *Proc. Natl. Acad. Sci. U.S.A.* **2014**, *111*, 1927−1932.
(36) Hu, C.; Cheng, L.; Wang, Z.; Zheng, Y.; Bai, S.; Qin, Y. A Transparent Antipeep Piezoelectric Nanogenerator to Harvest Tapping Energy on Screen. *Small* **2016**, *12*, 1315−1321.

https://dx.doi.org/10.1021/acsami.0c16973
ACS Appl. Mater. Interfaces 2020, 12, 54991−54999